EVS30 Symposium
Stuttgart, Germany, October 9 - 11, 2017

Modelling and Evaluation of Battery Packs with Different Number of Paralleled Cells

Fengqi Chang[1, 2], Felix Roemer[1, 2], Michael Baumann[2], Markus Lienkamp[1, 2]

1. TUM CREATE Ltd., 1 CREATE Way, #10-02 CREATE Tower, Singapore 138602

2. Institute of Automotive Technology, Technical University of Munich

Summary

To better evaluate the configuration of battery packs in electric vehicles (EV) in the early design phase, this paper proposes a mathematic model for the simulation of battery packs based on the elementwise calculations of matrices. This model is compatible with the different battery models and has a fast simulation speed. An experimental platform is built for the verification. Based on the proposed model and the statistic features of battery cells, the influence of the number of paralleled cells in a battery pack is evaluated in Monte-Carlo experiments. The simulation results obtained from Monte-Carlo experiments show that the parallel number is able to influence the total energy loss inside the cells, the energy loss caused by the balancing of the battery management system (BMS) and the degradation of the battery pack.

Keywords: battery model, prediction, simulation, efficiency, state of charge

1 Introduction

The production technology of battery cells nowadays has greatly progressed, but the unevenness of the cell properties, e.g., the capacity, the inner resistance and the polarization time constants, between different cells is still inevitable [1], [2]. The evenness of cells will certainly result in extra charging and discharging processes when the cells are connected in a battery pack. For the paralleled cells in the pack, due to the difference of the polarization time constants and the inner resistance, a self-balancing process between cells can be observed after a charge or discharge [3–6]. For the cells in series, the cells with higher capacity will have a higher state of charge (SOC) than the average value during the operation of the battery pack. The extra SOC in those cells must be dissipated by the passive or active balancing of a battery management system (BMS) to prevent the over charge or over discharge of the weak cells [2], [7]. As these additional cycling of the batteries cannot be eliminated due to the unevenness of the cell properties, it is important to understand how the configuration of battery packs can influence those additional processes and how these additional processes can influence the electric and degradation behaviour of a battery pack. This knowledge can help to find a better configuration of a battery pack for different applications in an early design phase. In this paper, the focus is the impact caused by paralleling more cells of the same type in a battery pack.

Previous researchers also noticed the importance of the parallel number and the additional charging or discharging processes in the battery pack. The conclusions, however, are different. [8] compared the degradation behaviours of a battery pack and a single cell in an experiment, in which the high quality and homogenous cells were used, and no obvious difference was identified between a single cell and the battery

pack in the degradation test. [6], [9] concluded that a significant accelerated degradation can be observed when the capacities or resistances of two paralleled cells are largely different from each other. And the conclusion of [5] is that when the difference of inner resistances and capacities between cells is large, connecting more cells in parallel can reduce the stress on each individual cell and therefore decelerate the degradation of the whole battery pack.

One possible explanation to the contradiction of those conclusions in different tests is that all the aforementioned studies largely depended on the results obtained from a limited number of samples, a coincidence in which could thus be taken as the conclusion for the whole population. Secondly, all the conclusions were drawn based on the comparison between only one battery pack with a specific configuration and a single cell. The difference of the conclusions could be caused by the difference of the battery pack configurations. Therefore, in order to obtain a more general view of the influence of the parallel number, a statistic approach should be taken in the research and a large number of different battery packs should be tested.

However, testing a large number of battery packs in experiments is too time-consuming and ineffective in terms of cost. An efficient method to simulate battery packs is thus required. [3, 4] used Simulink to simulate the current distribution between paralleled cells, but expanding the model to thousands of interconnected cells is difficult, as every cell in the battery pack needs to be set and connected manually in the software. [3] built a model of a battery pack based on the models of the cells in the complex frequency domain. This model can be easily expanded to simulate large battery packs, but it contains a time-consuming iteration and therefore not suitable for large scale simulations or degradation simulations.

To enable the quick evaluation of battery packs while taking the statistic view, this paper firstly proposes a model of battery pack based on the elementwise calculation of matrices, in which different cell models can be implemented. Experimental results are obtained for the verification. Then the distributions followed by the properties of battery cells are obtained from the measurement results of 50 NCR18650PF cells. Based on the model and the statistic features of NCR18650PF cells, different battery packs are generated and simulated in Monte-Carlo experiments with the focus on how the number of cells in parallel can influence the efficiency and the degradation of battery packs.

2 Battery Pack Model

To build the battery pack model, this paper uses a second-order cell model [3] in Figure 1. The resistor $R_{0j,k}$ is the DC inner resistance. The open circuit voltage (OCV) $e_{j,k}$ is generated according to the state of charge ($SOC_{j,k}$). $i_{j,k}$ is the output current of the cell while the terminal voltage is denoted by $u_{j,k}$. Two RC circuits are used to demonstrate the polarization during charge or discharge. The four parameters, $R_{1j,k}$, $C_{1j,k}$, $R_{2j,k}$, $C_{2j,k}$, can be identified by measuring the transient voltage when the cell is discharged by a constant current. $R_{1j,k}$ and $C_{1j,k}$ are denoted to have a smaller time constant than that of $R_{2j,k}$ and $C_{2j,k}$, so that the polarization in the short term (several seconds) and the long term (several hours) can be demonstrated by $R_{1j,k}$, $C_{1j,k}$ and $R_{2j,k}$, $C_{2j,k}$ respectively.

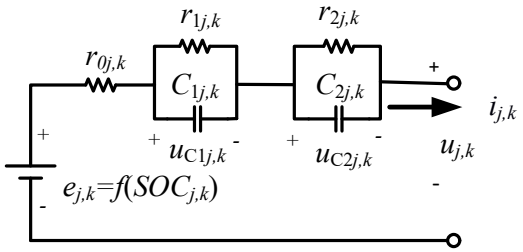

Figure 1: Equivalent circuit of a battery cell in the parallel row j and the column k

For a battery pack composed of n cells in parallel and m rows of paralleled cells connected in series (represented by npms thereafter in this paper), the quantity in Figure. 1 with subscript j,k means the properties of the cell in the jth parallel row and the kth column of the pack. $Q_{j,k}$ is the capacity of the corresponding cell. The output current of the pack is represented by i_{pack}. The output of the model is the current and the voltage of each cell in the battery pack when the load of the battery pack, i_{pack}, is given.

To calculate the output variables with a given input, paralleled cells in one row are analysed first. In a given row, e.g., the *j*th row, since all the battery cells are connected in parallel, the terminal voltage of the cells is the same, denoted by u_j. Using Kirchhoff's law of current, the following group of equations can be derived in eq. (1):

$$\begin{cases} i_{\text{pack}} = i_{j,1} + i_{j,2} + \ldots + i_{j,n} \\ u_j = e_{j,k} - u_{C1j,k} - u_{C2j,k} - R_{0j,k} i_{j,k} (k = 1, 2, \cdots, n) \end{cases} \tag{1}$$

In eq. (1), by transforming the cell terminal voltage equations into the cell current equations and then substituting all the cell current values in the pack current equation, eq. (2) can be obtained. The u_j and correspondingly the current of each cell can be calculated by eq. (2) if the polarization voltage and OCV are known.

$$\begin{cases} i_{\text{pack}} = \sum_{k=1}^{n} \dfrac{e_{j,k} - u_{C1j,k} - u_{C2j,k}}{R_{0j,k}} - u_j \sum_{k=1}^{n} \dfrac{1}{R_{0j,k}} \\ i_{j,k} = (e_{j,k} - u_{C1j,k} - u_{C2j,k} - u_j) / R_{0j,k} (k = 1, 2, \cdots, n) \end{cases} \tag{2}$$

However, the OCV and polarization voltage are state variables in this model, which cannot be calculated directly with only the information at a given point of time. Equations of state should thus be built to continue the modelling of the battery pack. Using the integer l to represent the lth step of the simulation, assuming that the initial SOC values of all the cells are already known, and that the polarization voltage of all the cells is zero initially, the equations of state in eq. (3) can be obtained. Δt is the time step of the simulation. In each step, four state variables, the SOC, the OCV and the polarization voltage values are updated first. Then the current distribution within the paralleled cells in the *j*th row and the cell voltage are recalculated, which will be used to update the state variables in the next simulation step. For the battery cells in other rows, the results could be obtained by sweeping the subscript j from 1 to m. In this way, the current and voltage of all the cells in the *n*p*m*s battery pack can be obtained. And it should be noted that the assumptions in this model are common in reality, because most battery tests should start at a known SOC value and after a long time of relaxation to eliminate the polarization voltage. Therefore, the model in eq. (3) can be reliably used to simulate a battery pack.

$$\begin{cases} SOC_{j,k}(l) = SOC_{j,k}(l-1) - \dfrac{i_{j,k}(l-1)\Delta t}{Q_{j,k}} \\ u_{C1j,k}(l) = \dfrac{i_{j,k}(l-1)R_{1j,k}\Delta t + u_{C1j,k}(l-1)R_{1j,k}C_{1j,k}}{\Delta t + R_{1j,k}C_1} \\ u_{C2j,k}(l) = \dfrac{i_{j,k}(l-1)R_{2j,k}\Delta t + u_{C2j,k}(l-1)R_{2j,k}C_{2j,k}}{\Delta t + R_{2j,k}C_{2j,k}} \\ e_{j,k}(l) = f(SOC_{j,k}(l)) \\ u_j(l) = \dfrac{\sum_{k=1}^{n} \dfrac{e_{j,k}(l) - u_{C1j,k}(l) - u_{C2j,k}(l)}{R_{0j,k}} - i_{\text{pack}}(l)}{\sum_{k=1}^{n} \dfrac{1}{R_{0j,k}}} \\ i_{j,k}(l) = [e_{j,k}(l) - u_j(l) - u_{C1j,k}(l) - u_{C2j,k}(l)] / R_{0j,k} \end{cases} \tag{3}$$

$k = 1, 2, \cdots, n$

$j = 1, 2, \cdots, m$

Initial conditions:

$SOC_{j,k}(0)$known

$u_{C1j,k}(0) = u_{C1j,k}(0) = 0$

$i_{j,k}(0) = 0$

As the model has no nonlinearly coupled variables, the model can be rewritten as the elementwise calculations of matrices as in eq. (4), in which all the operations of matrices are elementwise operations. Compared to calculating each variable in loops, the transformation (also known as vectorisation) of the

model can significantly improve the calculation speed if the Intel Math Kernel Library (MKL) is implemented in the simulation environment [10]. An example of such a simulation environment is MATLAB. On an Intel i7 6600U CPU, using this model on MATLAB, a simulation, in which a 72p108s (the configuration of the battery pack in Tesla Model S) battery pack discharged by a fluctuating load for 1800 s (time step 0.1 s) and then left stand for relaxation for another 800 s, is finished in 51.87 s.

$$
\begin{cases}
\mathbf{SOC}(l) = \mathbf{SOC}(l-1) - \dfrac{\mathbf{I}(l-1)\Delta t}{\mathbf{Q}} \\
\mathbf{U}_{\mathrm{C1}}(l) = \dfrac{\mathbf{I}(l-1)\bullet\mathbf{R}_1\Delta t + \mathbf{U}_{\mathrm{C1}}(l-1)\mathbf{R}_1\bullet\mathbf{C}_1}{\Delta t + \mathbf{R}_1\bullet\mathbf{C}_1} \\
\mathbf{U}_{\mathrm{C2}}(l) = \dfrac{\mathbf{I}(l-1)\bullet\mathbf{R}_2\Delta t + \mathbf{U}_{\mathrm{C2}}(l-1)\mathbf{R}_2\mathbf{C}_2}{\Delta t + \mathbf{R}_2\bullet\mathbf{C}_2} \\
\mathbf{E}(l) = f(\mathbf{SOC}(l)) \\
u_j(l) = \dfrac{\sum_{k=1}^{n} \dfrac{e_{j,k}(l) - u_{\mathrm{C1}j,k}(l) - u_{\mathrm{C2}j,k}(l)}{R_{0j,k}} - i_{\mathrm{pack}}(l)}{\sum_{k=1}^{n} \dfrac{1}{R_{0j,k}}} (j = 1, 2, \cdots, m) \\
\mathbf{I}(l) = [\mathbf{E}(l) - u_j(l) - \mathbf{U}_{\mathrm{C1}}(l) - \mathbf{U}_{\mathrm{C2}}(l)] / \mathbf{R}_0
\end{cases}
\tag{4}
$$

Initial conditions:

$\mathbf{SOC}(0)$known

$\mathbf{U}_{\mathrm{C1}}(0) = \mathbf{U}_{\mathrm{C2}}(0) = \mathbf{0}$

$\mathbf{I}(0) = \mathbf{0}$

It should also be noted that the second-order cell model used in this paper can be replaced by other detailed cell models for different purposes of research. The derivation procedure of the battery pack model in this paper still applies. The proposed battery pack model is more of a calculation framework than a fixed model and thus can be easily used by other researchers with different focuses.

3 Experimental Verification of the Proposed Model

In order to verify the model, an experiment platform was built (Figure 2). This platform is used to measure and record the current and voltage of four paralleled battery cells when they are discharged or charged. The parameters of the cells have been identified before the tests. And the line resistance of the circuit is measured accurately by a Kelvin bridge.

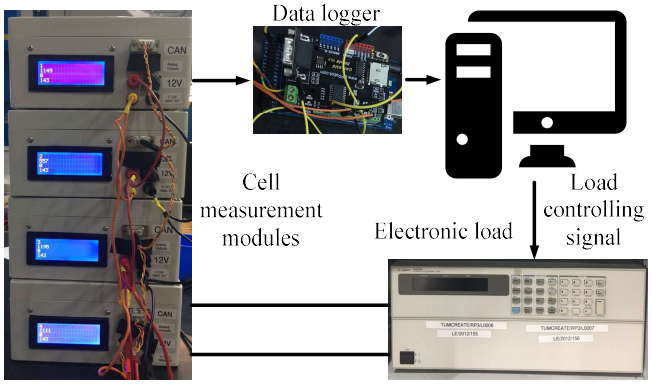

Figure 2: Experimental Platform to test paralleled battery cells

The four paralleled cells are firstly tested by a 1 C constant current load, starting from 80 % SOC until 20 % SOC. The current are recorded for another 2500 s after the removal of the load. The measured and simulated current waveforms of each cell are compared below in Figure 3. The simulated waveforms

follow the measured waveforms accurately. The maximum error of the simulation result is 0.06 A, still within 0.1 A, and it is found in the simulation result of the cell 1.

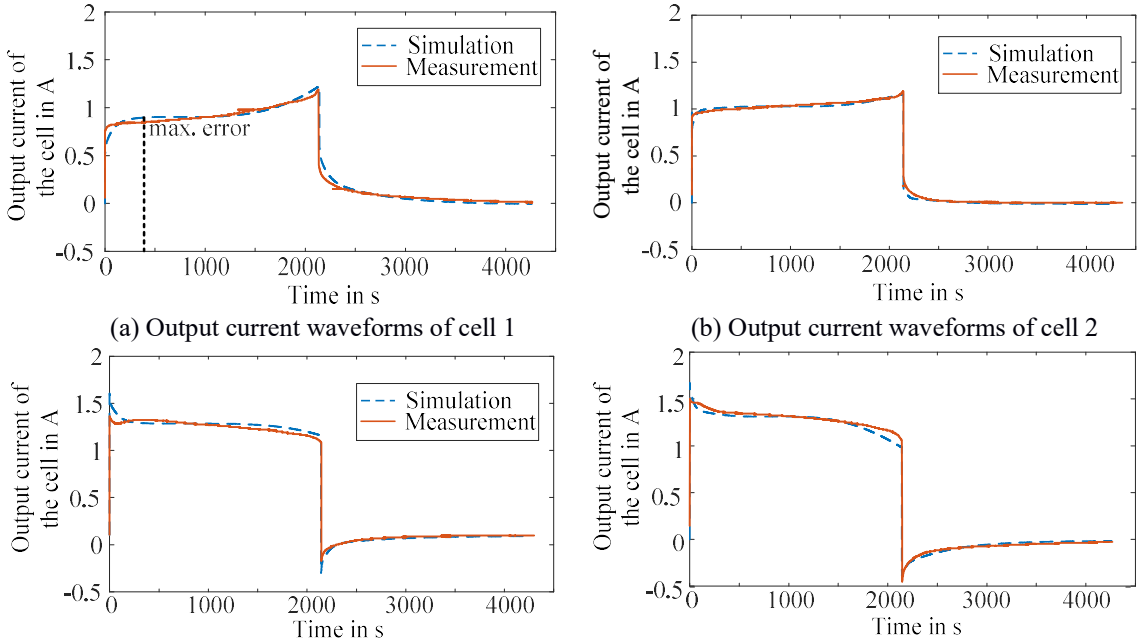

(a) Output current waveforms of cell 1

(b) Output current waveforms of cell 2

(c) Output current waveforms of cell 3

(d) Output current waveforms of cell 4

Figure 3: The simulated and measured current waveforms of four paralleled cells when discharged by the 1C constant current load

To evaluate the accuracy of the model in the automotive use cases, the four cells are also discharged by the C-rate curve in Figure 4. From 0 to 1800 s, the curve is the output current (in C-rate) of a battery pack in an EV, when the EV is simulated by the WLTP C3 driving cycle. The following 800 s is the relaxation period of the battery pack, during which the self-balancing current between paralleled cells can be observed. Therefore, this load C-rate curve is able to manifest the possible fluctuations of a practical load in an EV. The current waveforms in the simulation and the experiment are compared in Figure 5. The simulation and measured results can match accurately during the whole period of the test. The maximum error, 0.39 A, appears in the simulation result of the cell 1 in the 1716th second, while the error of all the four cells in the remaining time is within 0.1 A.

Therefore, with the two tests it is proved that the proposed model is able to accurately calculate the current distribution within paralleled cells. The further results based on the models can thus also be reliable. The error observed in the simulation results of the cell 1 could be caused by the errors in the parameter identification.

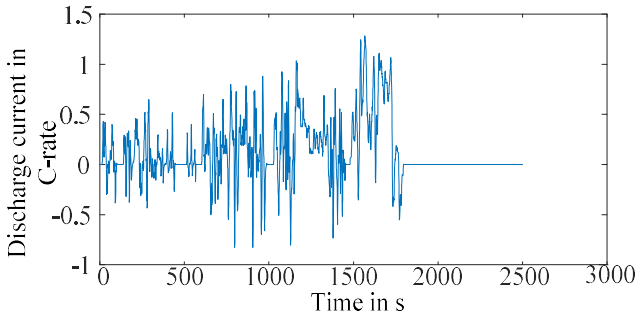

Figure 4: C-rate curve of the load current obtained in a simulation with the WLTP C3 driving cycle

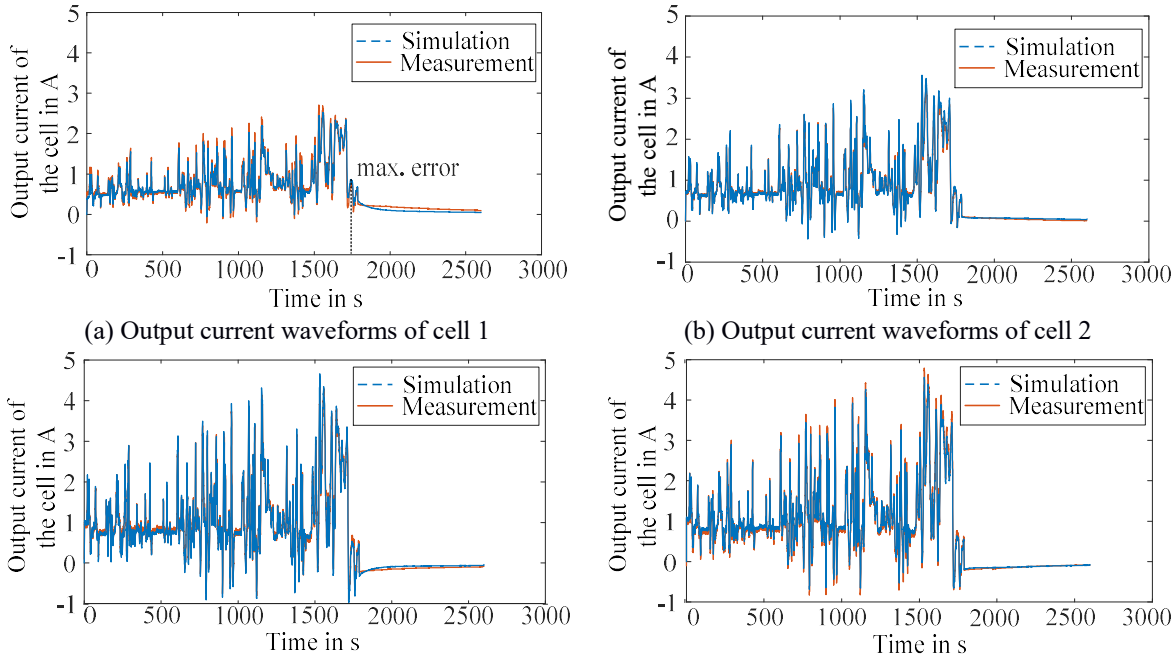

(a) Output current waveforms of cell 1

(b) Output current waveforms of cell 2

(c) Output current waveforms of cell 3

(d) Output current waveforms of cell 4

Figure 5: The simulated and measured current waveforms of four paralleled cells when discharged by the fluctuating driving cycle load

4 Evaluation of Battery Packs Based on Monte-Carlo Experiments

In this chapter, the proposed battery pack model is used in Monte-Carlo experiments to evaluate battery packs with different numbers of parallel. For each configuration, hundreds of battery packs are simulated and the conclusion based on these results will thus not be influenced by possible coincidences of a limited number of samples.

This paper only intends to find out the influence of paralleling more NCR18650PF cells instead of trying to find the optimal cell size and the corresponding parallel number for a given battery pack capacity. Therefore, it should be noted that all the cells generated in this paper have the same nominal capacity and that the battery packs with different parallel numbers thus have different capacities.

4.1 Statistic Features of Battery Cells

In order to generate the properties of the battery cells, i.e., the inner resistance ($R_{0j,k}$), capacity ($Q_{j,k}$), polarization resistors ($R_{1j,k}$, $R_{2j,k}$) and polarization capacitors ($C_{1j,k}$, $C_{2j,k}$) in the Monte-Carlo experiments, the statistic features and the distributions of the parameters are analysed based on the measured data of 50 Panasonic NCR18650PF cells.

The distribution of the cell capacity is studied first. The frequency histogram of the capacity is in Figure 6(a). The Kolmogorov-Smirnov test (KS-test) shows the probability of the null hypothesis that the capacity data complies with a normal distribution is 66 %. As this probability cannot directly decide if the null hypothesis should be accepted, the skewness of the data is also calculated. The skewness 0.1941 and the histogram show that the data has a clear skew on the right side. Therefore, this paper proposes to use the skew normal distribution instead of the normal distribution to generate the capacity of cells [11]. The choice can be reasonable, because the cell capacity must not be lower than the nominal value in the datasheet, which could result in a tendency in the production to make the distribution of the cell capacity skew to the right side.

Secondly, the distribution of the inner resistance is discussed. The histogram is in Figure 6(b), which resembles the normal distribution better than that of the cell capacity. The skewness of the inner resistance

data is 0.11. Therefore, although the probability of the null hypothesis is 51 % in the Kolmogorov-Smirnov test, the normal distribution is still adopted for the inner resistance due to the lower skewness and the histogram.

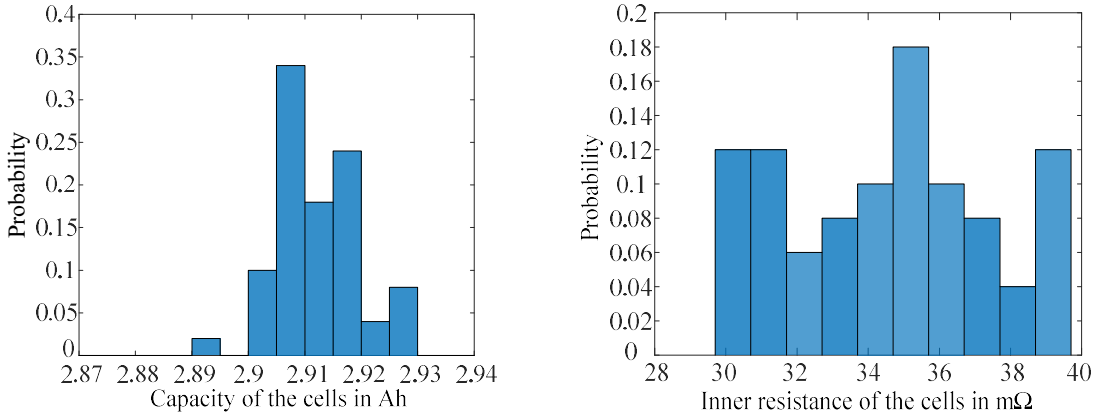

(a) Frequency histogram of the capacity (b) Frequency histogram of the DC inner resistance

Figure 6: The frequency histograms of the capacity and the inner resistance of the 50 cells

The four polarization parameters in the equivalent circuit, $R_{1j,k}$, $C_{1j,k}$, $R_{2j,k}$ and $C_{2j,k}$, are more difficult to measure, as there is no equipment specially designed for the automatic measurement of those parameters. Therefore, the polarization parameters of only 10 cells are identified manually to obtain their statistic features. As ten results cannot show an obvious pattern in the histograms, the statistic indices of the four polarization parameters are calculated to identify their distributions. Results are listed in Table I, in which the p-value of KS-test is the probability that the tested dataset complies with a normal distribution. From the p-values of the KS-test and the skewness values, it is seen that the $C_{2j,k}$ highly possibly follows the normal distribution while $R_{1j,k}$, $R_{2j,k}$ and $C_{1j,k}$ should be generated by skew normal distributions.

Table I Statistic indices of polarization indices

Indices	$R_{1j,k}$	$C_{1j,k}$	$R_{2j,k}$	$C_{2j,k}$
Mean	0.0122 Ω	326.6 F	0.06 Ω	1020.4 F
Standard Deviation	0.003 Ω	83.9 F	0.012 Ω	145.5 F
Skewness	1.0831	0.372	-0.9416	0.034
p-value of KS-test	0.441	0.628	0.539	0.902

Additionally, the interdependence between the six parameters should also be identified. The correlation between every two parameters is tested with the null hypothesis that the tested two parameters are linearly independent. Similar to a covariance matrix, the p-value (possibilities of the null hypothesis) of each test is listed in the symmetric matrix in Table II and located by the column and the row labelled by the two corresponding parameters. The values on the diagonal are not important, because they correspond to the self-dependence and must be 1. As all the p-values are lower than 50 %, the null hypothesises cannot be declined. The distributions of the parameters can be considered as linearly independent of each other.

Table II The matrix of p-values obtained from correlation tests of the six parameters

P-values of correlation tests	$Q_{j,k}$	$R_{0j,k}$	$R_{1j,k}$	$C_{1j,k}$	$R_{2j,k}$	$C_{2j,k}$
$Q_{j,k}$	1.00	0.04	0.21	0.22	0.33	0.10
$R_{0j,k}$	0.04	1.00	0.08	0.18	0.40	0.35
$R_{1j,k}$	0.21	0.08	1.00	0.00	0.18	0.00
$C_{1j,k}$	0.22	0.18	0.00	1.00	0.23	0.00
$R_{2j,k}$	0.33	0.40	0.18	0.23	1.00	0.31
$C_{2j,k}$	0.10	0.35	0.00	0.00	0.31	1.00

Based on the discussions above and the statistic indices, the properties of the cells in Monte-Carlo experiments could be generated by the distributions in eq. (5). $r_{0j,k}$ and $C_{2j,k}$ comply with normal

distributions, represented by N in eq. (5), while the other four properties are generated according to the skew normal distributions, represented by *SKEWN* in eq. (5).

In eq. (5), μ_1, μ_2 and σ_1, σ_2 are respectively the mean values and standard deviations of the two normal distributions. ω_1-ω_4, α_1-α_4 and ε_1-ε_4 are the parameters of the skew normal distributions. In the possibility density function (PDF) of the skew normal distribution, Φ and ϕ are respectively the cumulative distribution function (CDF) and the PDF of a standard normal distribution $N(0,1)$. The values of these parameters are selected to ensure that the distributions have the same mean values, standard deviations and skewness values as those of the measured data. The detailed values and calculation processes are not given in this paper due to the length limit.

$$\begin{cases} Q_{j,k} \sim SKEWN(\omega_1, \alpha_1, \varepsilon_1) \\ R_{0j,k} \sim N(\mu_1, \sigma_1^{\,2}) \\ R_{1j,k} \sim SKEWN(\omega_2, \alpha_2, \varepsilon_2) \\ C_{1j,k} \sim SKEWN(\omega_3, \alpha_3, \varepsilon_3) \\ R_{2j,k} \sim SKEWN(\omega_4, \alpha_4, \varepsilon_4) \\ \mathrm{C}_{2j,k} \sim N(\mu_2, \sigma_2^{\,2}) \end{cases} \tag{5}$$

in which

$$SKEWN(\omega, \alpha, \varepsilon) \sim PDF : \frac{2}{\omega}\phi(x)\Phi(\alpha(\frac{x-\varepsilon}{\omega}))$$

4.2 Simulative Evaluations with Monte-Carlo Experiments

Using the distributions in eq. (5), battery packs composed of randomly generated NCR18650PF cells are simulated to evaluate the influences of the parallel number.

Firstly, battery packs with 36p108s, 18p108s, 9p108s, 4p108s, 2p108s and 1p108s configurations are simulated to study the influence of the parallel number on the efficiency. The series connection number is constantly 108 to reach the required nominal voltage 400 V, while the parallel number starts at 36, half of the parallel number of the Tesla Model S battery pack, then declines following an equal ratio progression until 1 to make the difference brought by different parallel numbers more noticeable. The parallel number 9 is followed by 4 instead of 4.5, because the parallel number should be integer.

500 packs of each configuration are generated and simulated for one discharging cycle using the C-rate curve in Figure 4. In the single cycle simulation of each battery pack, the total energy dissipated by the BMS balancing and the total energy loss inside the cells are recorded. To obtain the proportions the two losses count in the total output, they are then divided by the net output energy of the battery packs. In that way, the losses of different battery packs can be compared. The medians, means, minimums and maximums of the proportions of the two losses over the parallel numbers are plotted in Figure 7(a) and (b).

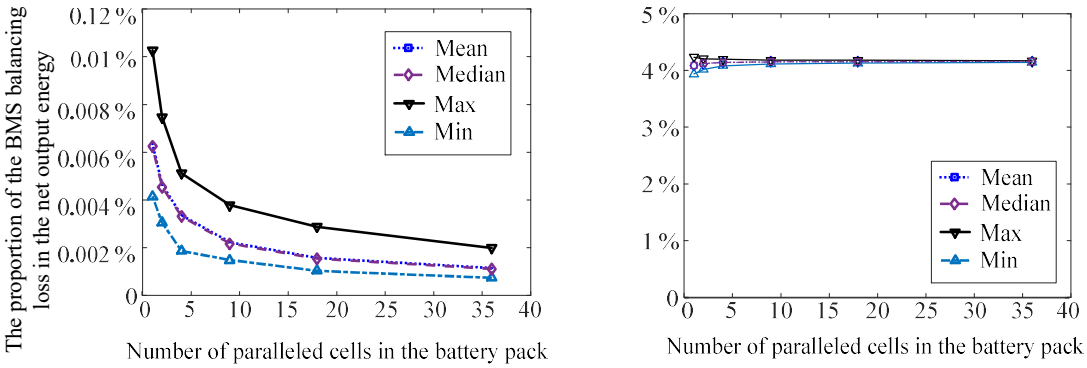

(a) The influence on the BMS balancing loss (b) The influence on the total in-cell energy loss

Figure 7: The influence of the parallel number on the losses of battery packs

Firstly it is observed that as the parallel number increases, the energy consumed by the balancing of BMS decreases. The reason is that the sum of several independent and identical distributions always has a lower relative standard deviation (standard deviation divided by mean value) compared to the original distribution as deduced in eq. (6). *SD* means standard deviation while the *E* is the expectation. Connecting more cells in parallel will lower the capacity difference between different rows of paralleled cells, and thus reduces the proportion of the energy consumed by the balancing of the BMS.

$$\begin{cases} SD(\sum_{i=1}^{N} X_i) / E(\sum_{i=1}^{N} X_i) = \dfrac{\sigma}{\mu\sqrt{N}} \\ SD(X_i) / E(X) = \dfrac{\sigma}{\mu} \\ X_1, X_2, ..., X_N \sim M(\mu, \sigma^2) \end{cases} \tag{6}$$

Secondly, an increasing number of paralleled cells is expected to result in a higher loss in the cells, because as the parallel number increases, a cell with the properties significantly different from those of the other cells in parallel is more likely to appear. This cell intensifies the energy exchanges between the cells and thus makes the energy loss inside the cells higher.

The curves of the maximum and minimum values manifest that the distribution of the total in-cell loss tends to converge as the parallel number increases in the Monte-Carlo experiments. Therefore, although the total in-cell loss tends to grow together with the parallel number, this loss is also more unlikely to diverge far from the expectation value.

However, the influence of the parallel number on the efficiency of a battery pack is not significant, as the changes of losses count lower than 0.1 % in the net output energy when the parallel number varies. Nonetheless, if the small influences accumulate over a longer time, it is possible that the aging behaviours of the battery packs are different.

Therefore, one battery pack with respectively 72p1s, 36p1s, 18p1s, 9p1s, 4p8s, 2p1s and 1p1s configuration is generated and simulated for 500 discharging cycles (the cycle life of Panasonic NCR18650PF cells) to observe the long term influence of the parallel number. In each cycle of simulation, the load curve in Figure 4 is repeated for 10 times to discharge the battery pack from 100 % SOC to 20 % SOC. The degradation model in [11] is used. Only one pack of each configuration is simulated, because of the long simulation time of the degradation test. And the series connection number of battery packs is reduced to one, because only the cells in parallel can influence each other in terms of degradation and one parallel row is thus already enough to demonstrate the aging behaviours. The simulation time is also in this way further reduced.

The simulation contains no temperature model and the temperature of the cells is set to be constantly 25 °C. Therefore, this simulation implies the assumption that the battery packs have a good cooling system to maintain the constant temperature. The statistic indices of the capacity and the inner resistance of all cells in each battery pack before and after the aging test are listed in Table III. The aging curves of the average capacity and the average inner resistance after every 100 cycles are plotted in Figure 8.

Firstly, the influence of the parallel number is more conspicuous in terms of degradation. In Table III it is observed that the highest increase of the mean inner resistance is 41.69 % in the 2p1s battery pack while the lowest increase is 39.77 % in the 1p1s battery pack (single cell). The difference is around 2 %.

Secondly, as the parallel number increases, instead of a monotonic trend, Figure 8(a) and (b) show that the changes of the average inner resistance and the average capacity tend to converge (to respectively around 40.7 % and -18.8 % in this paper) after 500 cycles of degradation test. The convergence is also supported by the standard deviations: When the parallel number is higher than 9, the post-test standard deviations of the capacity and the inner resistance of cells are significantly lower than those in the 2p1s and 4p1s packs, although the initial deviations of the 2p1s and 4p1s packs can be lower. That means the cell properties do not tend to diverge but to follow a consistent pattern when the parallel number is higher. The battery pack properties will thus also distribute in narrower intervals after the degradation test.

Table III The capacity and the inner resistance of cells in each battery pack before and after the degradation test

Configuration of battery packs		1p1s	2p1s	4p1s	9p1s	18p1s	36p1s	72p1s
New	$E(Q_{j,k})$	2.910 Ah	2.915 Ah	2.910 Ah	2.918 Ah	2.913 Ah	2.913 Ah	2.914 Ah
	$SD(Q_{j,k})$	-	0.0133	0.0058	0.0062	0.0073	0.0076	0.0082
	$E(r_{0j,k})$	38.16 mΩ	34.51 mΩ	34.91 mΩ	36.42 mΩ	35.64 mΩ	33.94 mΩ	34.26 mΩ
	$SD(r_{0j,k})$	-	0.0033	0.00451	0.00263	0.00242	0.00269	0.00284
After 500 cycles test	$E(Q_{j,k})$	2.372 Ah	2.361 Ah	2.362 Ah	2.367 Ah	2.365 Ah	2.365 Ah	2.365 Ah
	$E(Q_{j,k})$ change	-18.48 %	-19.02 %	-18.84 %	-18.89 %	-18.81 %	-18.82 %	-18.84 %
	$SD(Q_{j,k})$	-	0.0255	0.0301	0.0177	0.0113	0.0160	0.0185
	$E(r_{0j,k})$	53.33 mΩ	48.90 mΩ	49.00 mΩ	51.33 mΩ	50.10 mΩ	47.75 mΩ	48.22 mΩ
	$E(r_{0j,k})$ change	39.77 %	41.69 %	40.36 %	40.93 %	40.58 %	40.70 %	40.75 %
	$SD(r_{0j,k})$	-	0.00512	0.00513	0.00357	0.00308	0.00343	0.00352

Although only one pack of each configuration is simulated in the aging test, the trend of convergence can still be confirmed by the degradation of the battery pack properties and the cell properties. Therefore, it can be concluded that the degradation behaviour of battery packs with a higher parallel number is more consistent or, in other words, more predictable.

A possible explanation is that the energy exchange caused by the few particularly weak or strong cells is shared by more cells when the parallel number increases. The influence of these few cells on the aging of the battery pack degradation is thus limited.

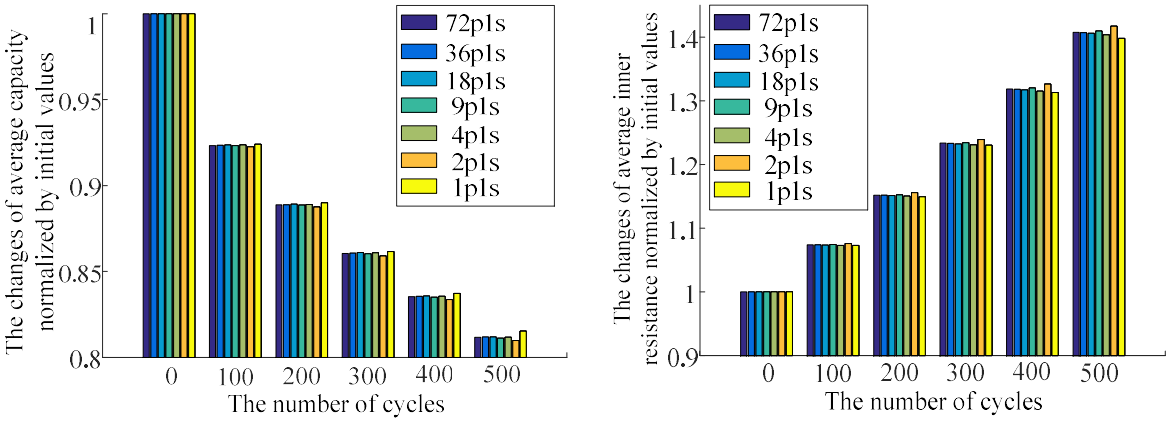

(a) Aging process of the average capacity (b) Aging process of the average inner resistance

Figure 8: The aging process of the average capacity and the average inner resistance of each battery pack

Another noteworthy phenomenon is that the degradation of the 1p1s battery pack (single cell) is slower than that of the other battery packs as seen in Figure 8. To verify if this is a coincidence of a single sample, another 15 single cells, i.e., 1p1s battery packs, are simulated. The maximum inner resistance growth and capacity reduction are respectively 40.31 % and -19.76 %, which are still lower than the corresponding changes of the other battery packs tested in this paper. Therefore, this phenomenon can be confirmed as a general situation. An explanation is that a single cell is not involved in any extra charging or discharging processes and thus has a lower cycle aging.

Based on the results collected in Monte-Carlo experiments, it can be concluded that the parallel number is able to influence the efficiency and the degradation of a battery pack. If the parallel number increases, the BMS balancing loss tends to decrease while the energy loss inside the cells tends to rise. However, when evaluating battery packs composed of homogeneous cells as in this paper, the influence on the efficiency is

only marginal. The influence on the degradation is in comparison more conspicuous. If more cells are paralleled in a battery pack, the degradation behaviours of the battery pack tend to be more predictable.

4.3 Discussion

As proved by the Monte-Carlo experiments, the parallel number cannot significantly influence the efficiency of a battery pack. The reason is that the significance is limited by the highly consistent cell properties, as all the distributions of the properties are obtained from the measurement results of high quality cells. If cells with higher variance are used to design a battery pack, the influence on efficiency should be considered.

Secondly, although the degradation simulation shows that the single cell has a slower aging process than that of the paralleled cells, it does not mean reducing the parallel number to one is an optimal choice. On the one hand there are more factors, e.g., the cost and reliability, need to be considered. On the other hand the degradation simulation largely depends on the degradation model and the temperature model. The conclusion could be changed if different models are selected to adapt to different scenarios of application.

Nonetheless, although the simulation in this paper does not have a temperature model and the universality of the conclusions could thus be limited, the proposed approach can still be used to further evaluate the configuration of battery packs in other scenarios by implementing more detailed or more specific models, because of the compatibility of the battery pack model.

5 Conclusion

The paper proposes a model for the simulation of battery packs, the accuracy of which is verified by experimental results. Using the proposed model and the statistic features of the battery cell properties, different battery packs are simulated in Monte-Carlo experiments to evaluate the potential influence of paralleling different numbers of the cells of the same type in a battery pack. When the parallel number changes, the influence on the degradation and the efficiency of the battery packs can be observed. The influence is not significant in term of efficiency because the cell properties have a high homogeneity. The influence on the degradation is in comparison more conspicuous. A higher parallel number will make the degradation behaviours of the battery packs more predictable.

The major contribution of this paper is the proposal of the battery pack model and the statistic approach to evaluate battery packs. In a practical design, if the statistical features of different battery cells are known, the proposed model and the approach can also be used to select the cells and correspondingly the configuration of the battery pack to achieve the best performance in terms of efficiency and degradation.

Acknowledgement:

This work was financially supported by the Singapore National Research Foundation under its Campus for Research Excellence And Technological Enterprise (CREATE) programme.

Contributions:

Mr. Fengqi Chang is the major author of the paper. He proposed the battery pack model and the approach to evaluate battery packs randomly generated cells in Monte-Carlo experiments. Mr. Felix Roemer designed the experimental platforms and conducted the verification experiments. Mr. Michael Baumann provided the capacity and inner resistance of the Panasonic NCR18650PF cells. Mr. Professor Markus Lienkamp made an essential contribution to the conception of the research project. He revised the paper critically for important intellectual content. Mr. Professor Markus Lienkamp gave final approval of the version to be published and agrees to all aspects of the work. As a guarantor, he accepts responsibility for the overall integrity of the paper.

References

[1] M. J. Brand, M. H. Hofmann, M. Steinhardt, S. F. Schuster, and A. Jossen, *Current distribution within parallel-connected battery cells*, J. Power Sources, vol. 334, pp. 202–212, 2016.

[2] X. Cui, W. Shen, Y. Zhang, C. Hu, and J. Zheng, *Novel active LiFePO4 battery balancing method based on chargeable and dischargeable capacity*, Comput. Chem. Eng., vol. 97, pp. 27–35, 2017.

[3] J. Zhang, S. Ci, H. Sharif, and M. Alahmad, *Modeling discharge behavior of multicell battery*, IEEE Trans. Energy Convers., vol. 25, no. 4, pp. 1133–1141, 2010.

[4] S. Miyatake, Y. Susuki, T. Hikihara, S. Itoh, and K. Tanaka, *Discharge characteristics of multicell lithium-ion battery with nonuniform cells*," J. Power Sources, vol. 241, pp. 736–743, 2013.

[5] X. Gong, R. Xiong, and C. C. Mi, *Study of the Characteristics of Battery Packs in Electric Vehicles with Parallel-Connected Lithium- Ion Battery Cells*, pp. 3218–3224, 2014.

[6] R. Gogoana, M. B. Pinson, M. Z. Bazant, and S. E. Sarma, *Internal resistance matching for parallel-connected lithium-ion cells and impacts on battery pack cycle life*, J. Power Sources, vol. 252, pp. 8–13, 2014.

[7] N. Bouchhima, M. Schnierle, S. Schulte, and K. P. Birke, *Erratum: Corrigendum to 'Active model-based balancing strategy for self-reconfigurable batteries'*, J. Power Sources, vol. 326, p. 226, 2016.

[8] C. Campestrini, P. Keil, S. F. Schuster, and A. Jossen, *Ageing of lithium-ion battery modules with dissipative balancing compared with single-cell ageing,* J. Energy Storage, vol. 6, pp. 142–152, 2016.

[9] W. Shi, X. Hu, C. Jin, J. Jiang, Y. Zhang, and T. Yip, *Effects of imbalanced currents on large-format LiFePO4/graphite batteries systems connected in parallel*, J. Power Sources, vol. 313, pp. 198–204, 2016.

[10] Intel, *Intel Math Kernel Library. Reference Manual*. 2003.

[11] J. Schmalstieg, S. Käbitz, M. Ecker, and D. U. Sauer, *A holistic aging model for Li(NiMnCo)O2 based 18650 lithium-ion batteries*, J. Power Sources, vol. 257, pp. 325–334, 2014.

Authors

Fengqi Chang obtained bachelor and master degree from Department of Electric Engineering, Tsinghua University, Beijing in 2013 and 2015. In July 2015 Fengqi Chang joined TUMCREATE as a research associate, working on the powertrains of electric vehicles. The research focus of Fengqi Chang is the efficiency modelling and improvement of electric powertrains. As the battery pack still counts more than half of the total price of an electric vehicle (EV). The improvement of efficiency can reduce the needed capacity of battery and, therefore, the cost of to raise the public acceptance of EVs.

Felix Roemer graduated from Technical University Munich as an Electrical Engineer in 2013 and since then is working for TUMCREATE in the team of "Individual Mobility Vehicle & Services" as a doctoral candidate. He was largely involved in the build-up of several, fully functional vehicle prototypes. His main work interests are in the area of fast implementing of electronic components for vehicle prototypes, micro mobility in general and batteries on a system level, where he investigates possibilities of new interconnections to increase overall efficiency.

Michael Baumann graduated from Technical University of Munich with a diploma degree in Mechatronics and Information Technology in 2013. Since then he is working at the Institute of Automotive Technology at TUM. During his work, he was largely involved in the build-up of several high voltage battery systems for stationary (e.g. EEBatt project) and mobile (e.g. EVA Taxi) applications. His research focuses on battery parameter estimation algorithms as well as battery lifetime estimation based on a coupling of electric-thermal and performance-based aging models.

Prof. Lienkamp (born in 1967) is conducting research in the area of electromobility with the objective of developing new vehicle concepts. He is professor of the Institute of Automotive Technology at Technical University of Munich (TUM) and is involved in the CREATE project in Singapore. After studying mechanical engineering at TU Darmstadt and Cornell University, Prof. Lienkamp obtained his doctorate at TU Darmstadt (1995). He worked at Volkswagen as part of an international trainee program and took part in a joint venture between Ford and Volkswagen in Portugal. Returning to Germany, he led the brake testing department in the VW commercial vehicle development section in Wolfsburg. He later became head of the "Electronics and Vehicle" research department in

Volkswagen AG's Group Research division. His main priorities were advanced driver assistance systems and vehicle concepts for electromobility. Prof. Lienkamp is heading the Chair of Automotive Technology at TUM since November 2009.